One-Step Preparation of Single-Crystalline β-MnO_2 Nanotubes

Deshan Zheng, Sixiu Sun,* Weiliu Fan, Haiyun Yu, Chunhua Fan, Guangxiang Cao, Zhilei Yin, and Xinyu Song

Key Laboratory of Colloid and Interface Chemistry, Shandong University, Ministry of Education, Jinan, Shandong 250100, People's Republic of China

Received: May 6, 2005; In Final Form: June 20, 2005

Single-crystal β-MnO_2 nanotubes with diameters in the range 200−500 nm and lengths up to several micrometers were successfully prepared by a simple hydrothermal method through oxidizing $MnSO_4$ with $NaClO_3$ in the presence of poly(vinyl pyrrolidone) (PVP). It was found that the formation process of β-MnO_2 nanotubes included two primary evolution stages over time: (1) the MnOOH nanoparticles initially formed in the hydrothermal system and anisotropic growth to nanorods and nanorod aggregates, and (2) the MnOOH nanorods transformed into β-MnO_2 tubular structure and grown into β-MnO_2 nanotubes due to continuous growth through a dissolution−recrystallization process eventually. Based on a series of experimental analysis, the formation mechanism of these nanostructures was discussed briefly. The present study has enlarged the family of nanotubes available and offers a possible new, general route to one-dimensional single-crystalline nanotubes of other materials.

1. Introduction

Nanoscale tubular structures have been the subject of intensive research throughout the world for their exceptional physical properties and potential applications in nanodevice technology. Since the discovery of carbon nanotubes,[1] there has being active interest in exploring other layered or nonlayered materials that form tubular structures. Various methods have been demonstrated to process a broad range of materials into nanotubes that have been summarized in several reviews;[2] typical examples include boron nitride,[3] metal dichalcogenides,[4] some metal oxides or hydroxides,[5] and a few metal nanotubes.[6] Our group also has now synthesized several types of nanotubes as well as titanium phosphate nanotubes and magnesium hydroxide nanotubes.[7] However, because of their unique structural characteristics, the preparation of nanotubes is relatively difficult, and fewer synthetic techniques have been developed compared with those for other one-dimensional nanostructures, such as nanorods and nanowires. The shape control and size tunability of these tubular nanostructures remain difficult and very laborious work to many researchers.

For many years, MnO_2 and derivative compounds have attracted special attention. Due to their outstanding structural flexibility combined with novel chemical and physical properties, they are widely used as catalysts, molecular sieves, and electrode materials in Li/MnO_2 batteries.[8] Moreover, well-controlled dimensionality, size, and crystal structure have also been regarded as critical factors that may bring some novel and unexpected properties, for example, isotropic or anisotropic behavior and region-dependent surface reactivity. Therefore, development of the morphologically controllable synthesis of MnO_2 nanoparticles is urgently important to answer the demand for exploring the potentials of manganese dioxide.[9] Over the past few years, remarkable process has been made in the synthesis of MnO_2 with different morphologies and different crystallographic forms. Nanorods and nanofibers of α-, β-, γ-, and δ-MnO_2 have been prepared by several research groups.[10] Very recently, a core−shell structure with spherically aligned nanorods was prepared in the case of α-MnO_2 by Xie and coworkers.[11]

Compared with nanorods, nanofibers, and core−shell structure, however, MnO_2 nanotubes are rarely reported. Although significant research endeavor has been devoted, there is still a lack of effective methods for production of high-quality MnO_2 nanotubes with precise morphological control. Ma et al.[12] first reported the production of manganese oxides nanotubes via a two-step procedure based on an ion intercalation/deintercalation process; nevertheless, the processing was clearly complicated and tedious. Wang and Li[13] also reported layer-structured curling δ-MnO_2 through an intercalation process about the same time. In addition, Wu et al.[14] have also used an electrochemical deposition method to fabricate MnO_2 nanotubes, but the electron diffraction (ED) patterns show them to be polycrystalline structures. Major synthetic difficulties encountered in this area are poor crystallinity, low yield, and process complexity. This attracted our interest to explore a simple, efficient method under mild conditions, and if a scheme is designed to produce the composites by one step instead of the above-mentioned two discrete processes or electrochemical deposition, then a safer and simpler preparation will be realized. This research work will be of great significance.

Herein, we introduce a facile and fast one-step solution-phase approach for the synthesis of β-MnO_2 nanotubes by oxidizing $MnSO_4$ with $NaClO_3$ in the presence of poly(vinyl pyrrolidone) (PVP). The nanotubes are very stable in ambient conditions after surface modification with PVP, a very important feat for future applications. To our knowledge, up to now, there have been no reports of β-MnO_2 nanotubes. Moreover, the possible formation mechanism of β-MnO_2 nanotubes has been proposed, which is speculated to follow a nucleation−dissolution−anisotropic growth−recrystallization mechanism.

10.1021/jp052370l CCC: $30.25
Published on Web 08/06/2005

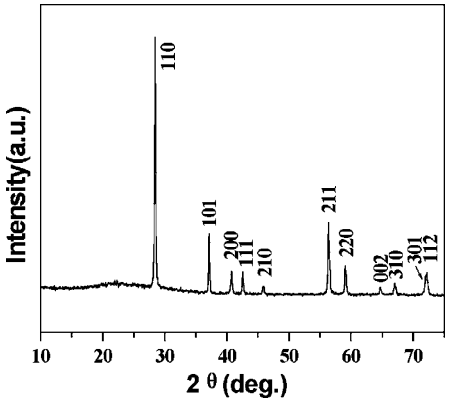

Figure 1. XRD patterns of as-synthesized β-MnO_2 nanotubes.

2. Experimental Section

2.1. Sample Preparation. β-MnO_2 nanotubes were synthesized under hydrothermal conditions. All chemicals were analytical-grade reagents and were used without further purification. In a typical process, 0.004 mol of $MnSO_4 \cdot H_2O$ was dissolved in 10 mL of distilled water and 0.0045 mol of PVP (K30, polymerization degree 360) was added slowly to it with vigorous stirring. When the solution clarified, 8 mL of aqueous solution containing 8 mmol of $NaClO_3$ was added to the above solution under continuous stirring. The resulting transparent solution was then transferred into a Teflon-lined stainless steel autoclave (20 mL) of 70% capacity of the total volume. The autoclave was sealed and maintained at 160 °C for 10 h. After the reaction was completed, the autoclave was allowed to cool to room temperature naturally. The solid black precipitate was filtered, washed several times with distilled water and absolute ethanol to remove impurities, and then dried at 50 °C in air. The obtained black powders were collected for the following characterization.

2.2. Characterization. The samples were characterized by X-ray diffraction (XRD) on a Japan Rigaku D/Max-γA rotating-anode X-ray diffractometer equipped with graphite-monochromatized Cu Kα radiation (λ = 1.541 78 Å) at a scanning rate of 0.02° s^{-1} in the 2θ range from 10° to 75°. The morphologies and nanostructure of the as-synthesized MnO_2 nanotubes products were characterized by field emission scanning electron microscopy (FESEM JSM-6700F). Transmission electron microscopy (TEM) was carried out on a JEOL 6300 at an accelerating voltage of 100 kV. The samples for these measurements were dispersed in absolute ethanol by vibration in the ultrasonic pool. Then, the solutions were dropped onto a copper grid coated with amorphous carbon films and dried in air before performance. More details about the structure of the 1D nanotubes were investigated by the selected area electron diffraction (SAED) pattern and high-resolution transmission electron microscopy (HRTEM) on a Hitachi 9000-NAR high-resolution transmission electron microscope, performed at 300 kV.

3. Results and Discussion

3.1. Composition of the Products. On the basis of the above solution-phase process, phase-pure tetragonal MnO_2 with pyrolusite structure could be obtained. Figure 1 shows an X-ray diffraction (XRD) pattern of as-synthesized β-MnO_2 nanotubes, and all the diffraction peaks can be readily indexed to the tetragonal phase of β-MnO_2 (Joint Committee on Powder Diffraction Standards [JCPDS] Card 24-0735: a = 4.399 Å, c = 2.874 Å). No peaks for other types or for amorphous MnO_2 were observed in the XRD patterns, indicating high purity and crystallinity of the final sample.

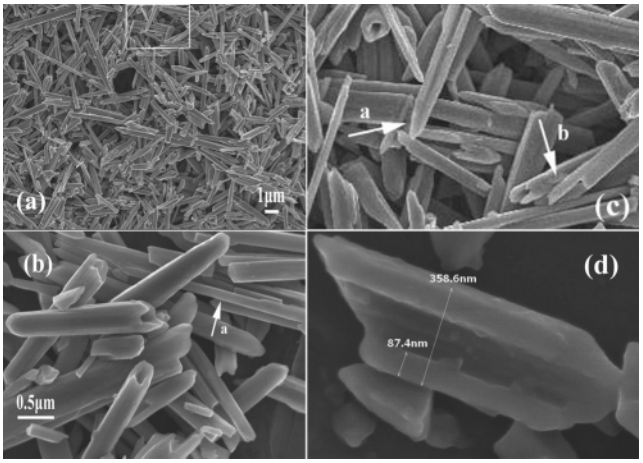

Figure 2. Characterizations of the tubular MnO_2 nanostructures formed by the hydrothermal process for 10 h. (a) Low-magnification SEM image of as-prepared β-MnO_2 nanotubes. (b) High-magnification SEM image of β-MnO_2 nanotubes. (c) Enlarged image of the portion indicated by the box in panel a. (d) Magnified view of one of the tubular crystals, revealing the hollow interior nature of these tubular structures.

3.2. Morphologies and Structures. The morphology and dimension of the as-prepared products were examined by scanning electron microscopy (SEM) (Figure 2). From the low-magnification SEM image (Figure 2a), one can see that the panoramic morphology of β-MnO_2 powder consists of rodlike crystals that are usually 200−500 nm in diameter and 1−6 μm in length and present in high quantity. Nevertheless, the SEM image at a higher magnification (Figure 2b) reveals that they have tubular structures. Figure 2c gives a partially magnified view of Figure 2a shows that one of the nanotubes' ends is round with a sharp tip and closed (arrow a); however, the tip openings are, in general, uneven, irregular, and sometimes present forklike (arrow b). After grinding or 10 min of ultrasonic treatment of the as-received products, many tubular structures were broken, as shown in Figure 2b,c (arrow a). Figure 2d gives a magnified view of one of the tubular crystals, revealing the hollow interior nature of these tubular structures. The diameter of the tubular crystal is around 358.6 nm and the thickness of the tube walls is estimated to be 87.4 nm.

The tubular structure of the products was further examined by TEM and HRTEM. Figure 3a shows a representative TEM image of a β-MnO_2 nanotube. The selected area electron diffraction (SAED) and HRTEM image of the β-MnO_2 nanotube are demonstrated in Figure 3 panels b and c, respectively. As indexed in Figure 3b, the SAED pattern was recorded from the [010] zone axis and has a highly symmetrical dotted lattice, which reveals the single-crystalline nature of tubular β-MnO_2. The lattice fringes in Figure 3c shows two sets of distinct lattice spacings of ca. 0.282 and 0.425 nm that correspond to the (001) and (100) planes of β-MnO_2, respectively. The axis of the nanotube was found to be parallel to the [001] direction, whereas the planes along the radial direction are [200] facets, indicating that the β-MnO_2 nanotube was grown along the [001] direction. Meanwhile, we can see from the images that the tubular nanostructures are structurally uniform and have no dislocations or other defects, along the growth direction. These clear lattice fringes in the HRTEM image further confirm the single-crystalline nature of the β-MnO_2 nanotubes.

3.3. Mechanism for the Formation of β-MnO_2 Nanotubes. It is well-known that the formation mechanism is very important

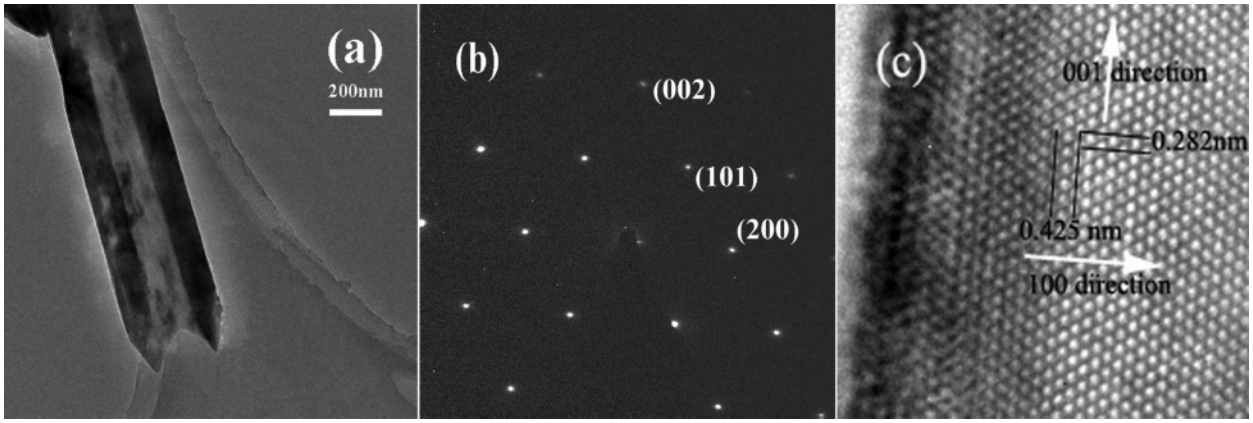

Figure 3. (a) Representative TEM image of the tubular MnO_2 nanostructures formed by the hydrothermal process for 10 h. (b) Corresponding SAED patterns of an individual β-MnO_2 nanotube. (c) HRTEM image of a part of the wall of a β-MnO_2 nanotube.

for exploring synthetic methods of nanotube formation. Concerning the formation mechanism for nanotubes, several models have been suggested; for instance, curving followed by seaming of molecular layers has been proposed to be responsible for the tube-formation process of materials with layered structure.[15] Direct growth through concentration depletion at the surfaces of cylindrical seeds has been suggested to explain the formation process of Te nanotubes containing chainlike building blocks,[16] and helical nanobelt−twist−join−growth has been suggested for the formation of Te nanotubes.[17] In the works of Ma et al.[12] and Wang and Li,[13], they regarded rolling as the mechanism for the conversion from nanosheets to nanotubes. In our system, however, no evidence is shown to support this hypothesis, for there are no manganese dioxide nanosheets or nanoplates observed in the formation of the present nanotubes process from our observations. The chemical reaction in the process to obtain β-MnO_2 nanotubes structures could be formulated as follows:

$$3Mn^{2+} + ClO_3^- + 3H_2O \rightarrow 3MnO_2 + Cl^- + 6H^+ \quad (1)$$

Based on our experimental process analysis, the reaction above can be divided into the two following steps:

$$6Mn^{2+} + ClO_3^- + 9H_2O \rightarrow 6MnOOH + Cl^- + 12H^+ \quad (2)$$

$$6MnOOH + ClO_3^- \rightarrow 6MnO_2 + Cl^- + 3H_2O \quad (3)$$

To study the formation mechanism of β-MnO_2 nanotubes, we have systematically surveyed the growth process of β-MnO_2 nanotubes by analyzing the samples at different growth stages. Figure 4 shows the TEM images of six samples taken at different stages of the hydrothermal reaction: (a) 2 h, (b) 2 h 20 min, (c) 3 h, (d) 5 h, (e) 8 h and (f) 10 h. The detailed growth process of the β-MnO_2 nanotubes may be described as follows: when the reaction had proceeded for 2 h, some nanoparticles were produced with diameters of 300−800 nm (Figure 4a). Then, after 20 min, some nanoparticles tended to attachment (inset of Figure 4b) and some nanorods were growing from the columnarlike nanoparticles (Figure 4b). When the reaction time is prolonged to 3 h, the intermediates of nanorods and nanorod aggregates can be observed. A typical nanorod aggregates is shown in Figure 4c. Meanwhile, the XRD analysis of these samples showed that they could be indexed to monoclinic MnOOH (see Supporting Information Figure S1a,b). Further observations showed that those nanorods and nanorod aggregates began to rupture from their cores in subsequent several minutes and finally were completely broken into independent nanorods

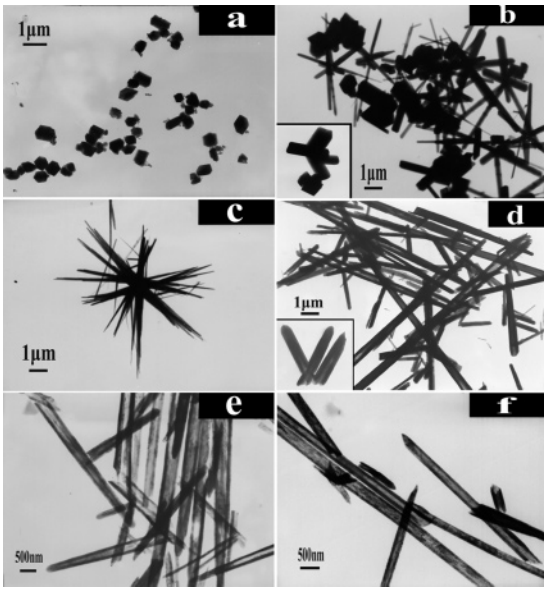

Figure 4. Set of TEM images corresponding to samples obtained at different growth stages of nanotubes after hydrothermal treatment for (a) 2 h, (b) 2 h 20 min, (c) 3 h, (d) 5 h, (e) 8 h, and (f) 10 h.

after 5 h of reaction (Figure 4d clearly demonstrates that). However, from a high-magnification image of the nanorods (inset of Figure 4d), it can be seen that the nanorods were not solid but some were tubelike. Correspondingly, the XRD pattern showed they were newly formed β-MnO_2 nanostructures and the peaks of monoclinic MnOOH have disappeared (see Supporting Information Figure S1c). When the reaction was lengthened to 8 h, relatively complete β-MnO_2 nanotubes were obtained with the opening tips, in general, uneven, irregular, and sometimes present forklike (Figure 4e). Under specific 10 h reaction, though the majority of nanotubes have round ends with sharp tips, and still some perfect β-MnO_2 nanotubes with diameters of 200−500 nm were formed (Figure 4f).

On the basis of the above observed morphologies and XRD patterns of products in different stages of evolution, it was possible to interpret the formation mechanism of the tubular structures as follows: First, some MnOOH nanoparticles were produced at a relatively slower rate according to the reaction in eq 2 when the reaction proceeded for 2 h. Meanwhile, some particles tended to attachment, and this attachment might be attributed to the destruction of the stabilization layer around each nanoparticle.[18] In addition, the aspect ratios of those nanoparticles make us believe that those nanoparticles just began to grow. Second, some nanoparticles as well as some attached

nanoparticles, as shown in Figure 4b, had, indeed, grown into rod-shaped anisotropic nanostructures with the assistance of PVP. On the basis of a series of experimental observations, we found that the volume of the nanoparticles was very small at the initial stages. Once the nuclei had been formed, the morphology of the nanoparticles changed very quickly from particles to nanorods and nanorod aggregates. In this period, we think the source of the MnOOH molecules for the growth of the nanorods come from two aspects: the reactants of the solution on one side, and the dissolution of the nanoparticles on the other side. With the rapid growth of nanorods and nanorod aggregates, the concentration of the reactants decreased, and then the dissolution process became dominant. Third, as the reaction proceeded, the MnOOH molecules slowly transformed into MnO_2 according to the reaction in eq 3, at this stage, nanorod aggregates began to rupture from their cores and evolved its morphology into tubelike nanorods; this was due to the formation of MnO_2 proceeding very slowly, which could not provide enough MnO_2 molecules for the growth of the growing rodlike crystals; this would lead to undersaturation in the central part of the growing regions of the rodlike nanoparticles,[19] and then the rodlike intermediate transformed into the tubular structure after continuous growth through a dissolution−recrystallization process.[20] At last, the nanotubes were formed due to the hydrothermal process providing sufficient energy for the dissolution and recrystallization of these rodlike crystals. In addition, the transition of nanorods into nanotubes indicates that the rods and nanorod aggregates and tubelike nanorods are intermediate states between small nanoparticles and nanotube states, but they are not in a metastable state, as this transformation happens only in the reaction solution. We found that the rods and nanorod aggregates and tubelike nanorods make no change at all after being kept in atmosphere over 3 months when they were separated from solvents, showing that they are stable. On the basis of the above discussions, it sounds reasonable to conclude that the reactions follow a nucleation−dissolution−anisotropic growth−recrystallization mechanism. A similar mechanism of nucleation−dissolution−recrystallization, suggested by Qian and co-workers,[21] has been accounted for the formation of Te nanotube. Certainly, this mechanism proposed needs to be confirmed by more studies.

It is well-known that using a polymer-assisted reaction to control the nucleation and growth is a simple but effective method, and some recent research has indicated that the capping organic molecules in the reaction system could modulate the kinetics of the crystal growth and determine the subsequent morphology of the product.[22] To further understand the nature of poly(vinyl pyrrolidone) (PVP) influencing the formation of β-MnO_2 nanotubes, varying amounts of the capping reagent PVP were used under the same synthesis conditions (Figure S2 in Supporting Information). It was found that, without PVP, only nanorods were produced. In the presence of a low concentration of PVP (0.05 mol/L), the products obtained were still rodlike. Increasing the polymer concentration from 0.1 to 0.3 mol/L resulted in the formation of the tubular β-MnO_2 nanotubes. The optimal concentration of PVP is about 0.25 mol/L to obtain uniform single-crystal nanotubes shown in Figure 2. As the PVP concentration was further increased to 0.5 mol/L, the tubular structures and solid nanorods coexisted with short rods in the system. Obviously, the concentration of PVP in our system is very important for causing a large difference among the growth rates of various crystallographic surfaces. Several recent studies have showed that the existence of an appropriate amount of capping reagents can alter the surface energies of various crystallographic surfaces to promote selective anisotropic growth of nanocrystals.[23] For the current system, due to the adsorption effect of PVP, the β-MnO_2 nanotubes can be prepared under specific reaction conditions. According to the above-mentioned experimental phenomena, we speculate that PVP was a structure-directing agent for the preparation of the β-MnO_2 nanotubes. Although the exact formation and growth mechanisms of β-MnO_2 nanotubes still need further investigation, our experimental results indicated that the PVP played crucial roles in controlling the morphologies of β-MnO_2 nanotubes. Meanwhile, other factors, such as reaction temperature, reaction time, and the molar ratio of $NaClO_3$ to $MnSO_4$, have important influences on the formation of β-MnO_2 nanotubes, and their effect on sample size and shape will be discussed in the future.

4. Conclusions

In summary, we have demonstrated a simple solution-phase approach to synthesis of single-crystalline β-MnO_2 nanotubes by oxidizing $MnSO_4$ with $NaClO_3$ in the presence of PVP. The capping molecules in the reaction system have been found to play an important role in controlling the growth of β-MnO_2 nanotubes. The advantages of our method for synthesizing the β-MnO_2 nanotubes lie in its simplicity, cheapness, and mild reaction conditions, which may be extended to other kinds of hollow structures or tubelike oxides by selecting the proper reaction conditions. In ongoing experiments, we hope to investigate the properties and applications of this novel tubular morphology and the possibility of synthesizing other nanotubes.

Supporting Information Available: XRD patterns of samples obtained at different growth stages of nanotubes and TEM images of samples obtained with different concentration of PVP (PDF). This material is available free of charge via the Internet at http://pubs.acs.org.

References and Notes

(1) Iijima, S. *Nature* **1991**, *354*, 56.

(2) (a) Remškar, M. *Adv. Mater.* **2004**, *16*, 1497. (b) Hu, J.; Odom, T. W.; Lieber, C. M. *Acc. Chem. Res.* **1999**, *32*, 435. (c) Patzke, G. R.; Krumeich, F.; Nesper, R. *Angew. Chem., Int. Ed.* **2002**, *41*, 2446. (d) Tenne, R. *Chem. Eur. J.* **2002**, *8*, 5297. (e) Rao, C. N. R.; Nath, M. *Dalton Trans.* **2003**, *1*, 1.

(3) Chopra, N. G.; Luyken, R. J.; Cherrey, K.; Crespi, V. H.; Cohen, M. L.; Louie, S. G.; Zettl, A. *Science* **1995**, *269*, 966.

(4) (a) Tenne, R.; Margulis, L.; Genut, M.; Hodes, G. *Nature* **1992**, *360*, 444. (b) Feldman, Y.; Wasserman, E.; Srolovitz, D. J.; Tenne, R. *Science* **1995**, *267*, 222. (c) Nath, M.; Rao, C. N. R. *J. Am. Chem. Soc.* **2001**, *123*, 4841. (d) Nath, M.; Rao, C. N. R. *Angew. Chem., Int. Ed.* **2002**, *41*, 3451. (e) Brorson, M.; Hansen, T. W.; Jacobsen, C. J. H. *J. Am. Chem. Soc.* **2002**, *124*, 11582.

(5) (a) Hoyer, P. *Langmuir* **1996**, *12*, 1411. (b) Wu, J.; Liu, S.; Wu, C.; Chen, K.; Chen, L. *Appl. Phys. Lett.* **2002**, *81*, 1312. (c) Nakamura, H.; Matsui, Y. *J. Am. Chem. Soc.* **1995**, *117*, 2651. (d) Yada, M.; Mihara, M.; Mouri, S.; Kuroki, M.; Kijima, T. *Adv. Mater.* **2002**, *14*, 309. (e) Fang, Y. P.; Xu, A. W.; You, L. P.; Song, R. Q.; Yu, J. C.; Zhang, H. X.; Li, Q.; Liu, H. Q. *Adv. Funct. Mater.* **2003**, *13*, 955. (f) Xu, A. W.; Fang, Y. P.; You, L. P.; Liu, H. Q. *J. Am. Chem. Soc.* **2003**, *125*, 1494.

(6) (a) Hutleen, J. C.; Jirage, K. B.; Martin, C. R. *J. Am. Chem. Soc.* **1998**, *120*, 6603. (b) Tourillon, G.; Pontonnier, L.; Levy, J. P.; Langlais, V. *Electrochem. Solid-State Lett.* **2000**, *3*, 20. (c) Han, C. C.; Bai, M. Y.; Lee, J. T. *Chem. Mater.* **2001**, *13*, 4260. (d) Li, X.; Li, Y.; Li, S.; Zhou, W.; Chu, H.; Chen, W.; Li, I. L.; Tang, Z. *Cryst. Growth Des.* **2005**, *5*, 911. (e) Li, Y.; Wang, J.; Deng, Z.; Wu, Y.; Sun, X.; Yu, D.; Yang, P. *J. Am. Chem. Soc.* **2001**, *123*, 9904.

(7) (a) Yin, Z.; Sakamoto, Y.; Yu, J.; Sun, S.; Terasaki, O.; Xu, R. *J. Am. Chem. Soc.* **2004**, *126*, 8882. (b) Fan, W. L.; Sun, S. X.; You, L. P.; Cao, G. X.; Song, X. Y.; Zhang, W. M.; Yu, H. Y. *J. Mater. Chem.* **2003**, *13*, 3062.

(8) (a) Huang, H. M.; Mao, S.; Feick, H.; Yan, H.; Wu, Y.; Kind, H.; Weber, E.; Russo, R.; Yang, P. *Science* **2001**, *292*, 1897. (b) Armstrong, A. R.; Bruce, P. G. *Nature* **1996**, *381*, 499. (c) Ammundsen, B.; Paulsen, J. *Adv. Mater.* **2001**, *13*, 943.

(9) Wu, C.; Xie, Y.; Wang, D.; Yang, J.; Li, T. *J. Phys. Chem. B* **2003**, *107*, 13583.

(10) (a) Wang, X.; Li, Y. *Chem. Commun.* **2002**, *7*, 764. (b) Wang, X.; Li, Y. *J. Am. Chem. Soc.* **2002**, *124*, 2880. (c) Yuan, Z. Y.; Zhang, Z. L.; Du, G. H.; Ren, T. Z.; Su, B. L. *Chem. Phys. Lett.* **2003**, *378*, 349. (d) Al-Sagheer, F. A.; Zaki, M. I. *Colloids Surf. A.* **2000**, *173*, 193.

(11) Li, Z. Q.; Ding, Y.; Xiong, Y. J.; Yang, Q.; Xie, Y. *Chem. Commun.* **2005**, *7*, 918.

(12) Ma, R.; Bando, Y.; Sasaki, T. *J. Phys. Chem. B* **2004**, *108*, 2115.

(13) Wang, X.; Li, Y. D. *Chem. Lett.* **2004**, *33*, 48.

(14) Wu, M. S.; Lee, J. T.; Wang, Y. Y.; Wan, C. C. *J. Phys. Chem. B* **2004**, *108*, 16331.

(15) Ye, C.; Meng, G.; Jiang, Z.; Wang, Y.; Wang, G.; Zhang, L. *J. Am. Chem. Soc.* **2002**, *124*, 15180.

(16) Mayers, B.; Xia, Y. N. *Adv. Mater.* **2002**, *14*, 279.

(17) Mo, M. S.; Zeng, J. H.; Liu, X. M.; Yu, W. C.; Zhang, S. Y.; Qian, Y. T. *Adv. Mater.* **2002**, *14*, 1658.

(18) (a) Chen, J.; Herricks, T.; Geissler, M.; Xia, Y. *J. Am. Chem. Soc.* **2004**, *126*, 10854. (b) Chen, S.; Kimura, K. *J. Phys. Chem. B* **2001**, *105*, 5397.

(19) (a) Krueger, G. C.; Miller, C. W. *J. Chem. Phys.* **1953**, *21*, 2018. (b) Tang, Q.; Liu, Z. P.; Li, S.; Zhang, S. Y.; Liu, X. M.; Qian, Y. T. *J. Cryst. Growth.* **2003**, *259*, 208.

(20) (a) Lu, J.; Xie, Y.; Xu, F.; Zhu, L. Y. *J. Mater. Chem.* **2002**, *12*, 2755. (b) Chen, M.; Xie, Y.; Lu, J.; Xiong, Y. J.; Zhang, S. Y.; Qian, Y. T.; Liu, X. M. *J. Mater. Chem.* **2002**, *12*, 748.

(21) Xi, G.; Peng, Y.; Yu, W.; Qian, Y. *Cryst. Growth Des.* **2005**, *5*, 325.

(22) (a) Xia, Y.; Yang, P.; Sun, Y.; Wu, Y.; Mayers, B.; Gates, B.; Yin, Y.; Kim, F. *Adv. Mater.* **2003**, *15*, 353. (b) Sun, Y.; Xia, Y. *Adv. Mater.* **2002**, *14*, 833. (c) Sun, Y.; Yin, Y.; Mayers, B. T.; Herricks, T.; Xia, Y. *Chem. Mater.* **2002**, *14*, 4736. (d) Peng, X.; Manna, L.; Yang, W. D.; Wickham, J.; Scher, E.; Kadavanich, A.; Alivisatos, A. P. *Nature* **2000**, *404*, 59.

(23) (a) Peng, X. *Adv. Mater.* **2003**, *15*, 459. (b) Lee, S. M.; Cho, S. N.; Cheon, J. *Adv. Mater.* **2003**, *15*, 441. (c) Guo, L.; Liu, C.; Wang, R.; Xu, H.; Wu, Z.; Yang, S. *J. Am. Chem. Soc.* **2004**, *126*, 4530.